Zhang *et al. Chem Synth* 2024;4:39
DOI: 10.20517/cs.2023.74

Chemical Synthesis

Mini Review

Open Access

Crystal facet engineering of electrocatalysts for nitrate reduction to ammonia: recent advances and future perspectives

Yuwei Zhang, Hanfeng Liang*

State Key Laboratory of Physical Chemistry of Solid Surfaces, Tan Kah Kee Innovation Laboratory (IK K EM), Department of Chemical and Biochemical Engineering, College of Chemistry and Chemical Engineering, Xiamen University, Xiamen 361005, Fujian, China.

Correspondence to: Dr. Hanfeng Liang, State Key Laboratory of Physical Chemistry of Solid Surfaces, Tan Kah Kee Innovation Laboratory (IKK EM), Department of Chemical and Biochemical Engineering, College of Chemistry and Chemical Engineering, Xiamen University, Xiamen 361005, Fujian, China. E-mail: hfliang@xmu.edu.cn

How to cite this article: Zhang Y, Liang H. Crystal facet engineering of electrocatalysts for nitrate reduction to ammonia: recent advances and future perspectives. *Chem Synth* 2024;4:39. https://dx.doi.org/10.20517/cs.2023.74

Received: 29 Dec 2023 **First Decision:** 6 Mar 2024 **Revised:** 11 Apr 2024 **Accepted:** 18 Apr 2024 **Published:** 4 Jul 2024

Academic Editor: Xiang-Dong Yao **Copy Editor:** Pei-Yun Wang **Production Editor:** Pei-Yun Wang

Abstract

Ammonia (NH_3) is an important chemical feedstock and a clean energy carrier that has a pivotal impact on the sustainable energy circle. Its electrocatalytic production is evolving into a green alternative to the traditional Haber-Bosch process. A key strategy in enhancing the performance of this electrocatalytic ammonia synthesis is crystal facet engineering of electrocatalysts, which could significantly influence the reaction mechanism, kinetics, and thermodynamics. This review summarizes the recent advancements in crystal facet engineering for electrocatalytic nitrate reduction to ammonia. Through this review, we hope to shed light on the significant role of crystal facet engineering in advancing electrocatalytic ammonia production and provide useful guidance on the design of high-performance electrocatalysts.

Keywords: Nitrate reduction reaction, crystal facet engineering, electrocatalysts

INTRODUCTION

Ammonia (NH_3), as a key chemical in numerous industrial applications, has widespread usage as a primary raw material in manufacturing fertilizers[1], explosives, refrigerants, and pharmaceuticals. About 50% of the

nitrogen content in the human body comes from synthetic ammonia, indicating that ammonia is crucial to human beings and the global economy. Additionally, as a carbon-free energy carrier, ammonia possesses a high energy density of 3 $kWh \cdot kg^{-1}$. It serves as a viable option for direct liquid fuel utilization in electricity and power generation applications. This can be achieved by using direct ammonia fuel cells or catalytic ammonia combustion methods. Ammonia also can be used to store hydrogen with a high hydrogen capacity of 17.75 wt%[2]. Compared to hydrogen, it can be easily liquefied when compressed to 1 MPa at room temperature (298 K) or cooled to 240 K at ambient pressure (0.1 MPa), making it an ideal medium for the safe transportation and storage of hydrogen[3,4].

The global ammonia production is currently 170 million tonnes per year[5], mostly coming from the Haber Bosch process ($N_2 + H_2 \rightarrow NH_3$) that typically requires high temperatures (400-500 °C) and pressures (15-35 MPa)[6-8]. Although this process has been widely adopted in the industry, it is highly energy-intensive and consumes about 1.8% of the global energy production annually. In addition, approximately 500 million tons of CO_2 are emitted annually, considering that the hydrogen feedstock for the Haber Bosch process mainly comes from steam reforming of natural gas or coals[9]. Therefore, the development of "green ammonia" is crucial. Electrocatalytic nitrogen species reduction for ammonia production is considered a promising green ammonia production technology. In electrochemical reactions, electrons act as reducing agents, neither introducing any impurities nor adversely affecting the environment. Currently, many studies focus on electrocatalytic nitrogen reduction reaction (NRR)[10] [$N_2 + 6e^- + 6H_2O \rightarrow 2NH_3 + 6OH^-$, 0.09 V *vs.* reversed hydrogen electrode (RHE)], which drives the conversion of N_2 to ammonia under ambient conditions. However, the ammonia Faraday efficiency and yield of NRR are generally low due to the difficulty in breaking the extremely stable N≡N bonds (941 $kJ \cdot mol^{-1}$) and the low solubility of N_2 in aqueous electrolyte[11]. Instead, the electrocatalytic nitrate reduction reaction to ammonia (NtrRR) becomes a promising option since it is thermodynamically more feasible. The NtrRR has a positive theoretical electrode potential ($NO_3^- + 8e^- + 6H_2O \rightarrow NH_3 + 9OH^-$, 0.69 V *vs.* RHE) and, thus, can effectively avoid interference from competitive hydrogen evolution reaction (HER). In addition, breaking N=O bonds requires a much lower energy input (204 $kJ \cdot mol^{-1}$). Therefore, the Faraday efficiency and NH_3 yield of NtrRR are much higher than those of NRR[12].

However, the large-scale application of NtrRR still faces many challenges, such as high overpotential and low Faraday efficiency and ammonia yield, which are mostly associated with efficiency of the electrocatalysts. Therefore, many strategies, such as nanostructuring[13], doping[7,14,15], and alloying[16-18], have been explored to enhance the performance of electrocatalysts. Among them, crystal facet engineering is regarded as a highly effective approach since the crystal facet represents the most fundamental element of a nanostructure. It directly determines the surface atomic arrangement and orientation and, therefore, the adsorption and activation of the reactants and intermediates, which essentially determine the catalytic activity. Indeed, crystal facet engineering has shown the efficacy of enhancing the electrocatalyst performance towards not only the NtrRR but also many other electrocatalytic reactions, including HER, NRR, oxygen reduction reaction (ORR), and oxygen evolution reaction (OER)[19-21]. It is well acknowledged that high-index facets generally possess higher catalytic activity; however, they are thermodynamically unstable and, thus, are difficult to synthesize through common methods. While low-index facets, on the other hand, are much easier to synthesize, they could still significantly influence both the activity and stability of the catalysts. Therefore, understanding the relationship between the crystal facets and NtrRR performance is essential for the rational design of high-performance electrocatalysts.

In this review, we summarize the recent advances in crystal facet engineering of electrocatalysts for the NtrRR, focusing on the effects of different facets on the reaction mechanism, kinetics, and thermodynamics.

We also discuss the challenges and opportunities in this research field and provide some perspectives for future development.

REACTION MECHANISM OF NTRRR

Electrocatalytic nitrate reduction reaction is a complex multi-electron and multi-proton transfer process, and the final product exists in the form of chemically stable N_2 [Equation (1)] and/or NH_3 [Equation (2)]:

$$2NO_3^- + 10e^- + 6H_2O \rightarrow N_2 + 12OH^- \quad (1)$$

$$NO_3^- + 8e^- + 6H_2O \rightarrow NH_3 + 9OH^- \quad (2)$$

Depending on the specific conditions and catalysts, the reaction can follow either an indirect or a direct pathway[22,23]. The indirect pathway only occurs under conditions of NO_3^- concentration greater than 1 mol·L^{-1} and low pH. In this scenario, NO_3^- does not participate in electron transfer during the reduction process. The direct pathway, on the other hand, often proceeds at concentrations below 1 mol·L^{-1} and is the most widely reported mechanism in literature. In this pathway [Figure 1], nitrate reduction involves the adsorption of reactants and intermediates, followed by electron transfer. First, NO_3^- is adsorbed on the catalyst surface and then reduced to $^*NO_2^-$ through electron transfer [Equation (3)], which is typically considered as the rate-limiting step[22]. This is because $^*NO_2^-$ has a high energy of the lowest unoccupied molecular π^* orbital (LUMO π^*), which makes it difficult for charges to be injected into this orbital[11]. Next, $^*NO_2^-$ can rapidly react with protons on the electrode surface to produce $^*NO$. A fraction of $^*NO$ is then reduced to NH_3 [Equations (4) and (5)], while the rest is desorbed from the electrode surface to produce $^*NO$. Some of the NO(aq) form weakly adsorbed NO dimers, which further react to generate N_2O and ultimately convert to N_2.

$$^*NO_3^- + 2e^- + H_2O \rightarrow {}^*NO_2^- + 2OH^- \quad (3)$$

$$^*NO_2^- + e^- + H_2O \rightarrow {}^*NO + 2OH^- \quad (4)$$

$$^*NO + 5e^- + 4H_2O \rightarrow NH_3 + 5OH^- \quad (5)$$

In addition, the adsorbed NO_3 can also be reduced by the adsorbed $^*H$ that is generated by water dissociation through the Volmer process [Equation (6)][24]. The $^*H$ then participates in the reduction of intermediates (NO_3^-, $^*NO_2^-$, and $^*NO$) to $^*N$ [Equations (7)-(9)]. This process is known as $^*H$-mediated reduction, distinguished from the electron-mediated reduction discussed earlier. The $^*H$-mediated process would preferably form $^*NH_3$ as $^*H$-mediated N–H bonds are easier to form than N–N bonds [Equations (10)-(12)]. $^*NH_3$ then desorbs from the electrode surface to produce NH_3.

$$H_2O + e^- \rightarrow {}^*H + OH^- \quad (6)$$

$$NO_3^- + 2{}^*H \rightarrow {}^*NO_2^- + H_2O \quad (7)$$

$$^*NO_2^- + {}^*H \rightarrow {}^*NO + OH^- \quad (8)$$

$$^*NO + 2{}^*H \rightarrow {}^*N + H_2O \quad (9)$$

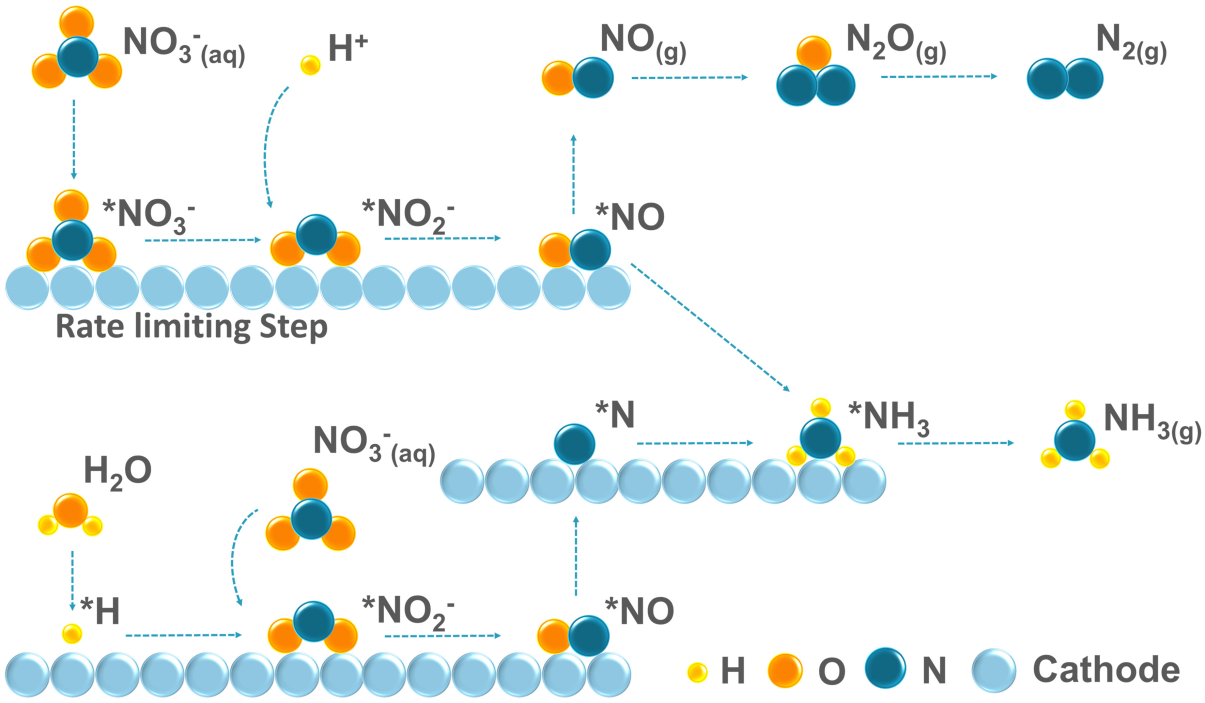

Figure 1. Electrochemical NtrRR mediated by electron transfer and atomic hydrogen.

$$^{*}N + {}^{*}H \rightarrow {}^{*}NH \quad (10)$$

$$^{*}NH + {}^{*}H \rightarrow {}^{*}NH_2 \quad (11)$$

$$^{*}NH_2 + {}^{*}H \rightarrow {}^{*}NH_3 \quad (12)$$

Resulting from the complex multi-electron coupled proton transfer process, NtrRR suffers from sluggish kinetics and low selectivity towards NH_3. The NtrRR performance highly depends on the properties of electrocatalysts, which determine the adsorption and activation of reactants and intermediates. Tremendous efforts have, therefore, been devoted to exploring efficient and stable electrocatalysts to promote the reaction kinetics and selectivity. Crystal facet engineering has emerged as a successful approach to boost the performance of electrocatalysts in various electrochemical reactions, including the HER, NRR[25-27], and ORR[19,20]. This is because the crystal facets determine the atomic configurations and, thus, the interactions between the surface active sites and reaction intermediates, resulting in improved reaction energetics.

CRYSTAL FACETS AND REGULATION STRATEGIES

A crystal facet is a plane that passes through any three points of the spatial lattice of a crystal, and it is denoted by the Miller index (*hkl*). Figure 2A shows a triangle diagram that illustrates the direct relationship between the shapes of polyhedra and the corresponding facets in a cubic crystal system[28]. The vertices of the triangle symbolize three common polyhedra enclosed by low-index facets: a cube with six (100) facets, an octahedron with eight (111) facets, and a rhombic dodecahedron with twelve (110) facets. The coordination numbers of the atoms on the outermost layer of the (111), (100), and (110) facets are 9, 8, and 7, respectively. The other crystal facets are referred to as high-index facets (*h*, *k*, *l* having at least one greater than 1). The edges of the triangle [(001), (110), (011) crystal zones] and its interior represent different facets.

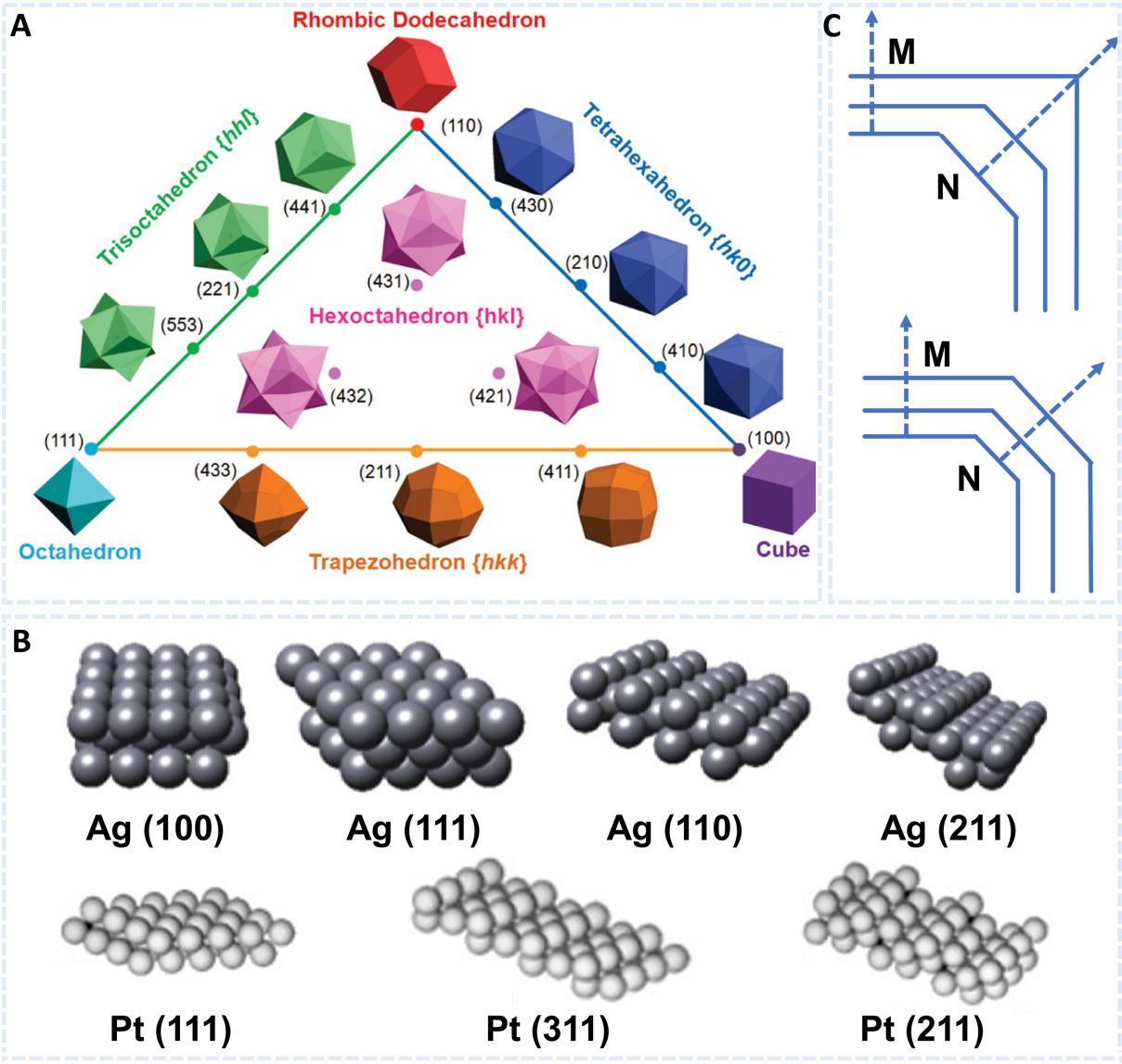

Figure 2. (A) Relationship between the shape of a crystal and its facets. Reproduced with permission[28]. Copyright 2010, American Chemical Society; (B) Surface atomic arrangement of Ag (100), (111), (110), (211) and Pt (311), (211) facets. Reproduced with permission[30,31]. Copyright 2015 and 2020, American Chemical Society; (C) Growth rates of specific facets determine the exposed surfaces.

These facets correspond to four types of high-index facet polyhedra: tetrahexahedron (THH), trapezohedron (TPH), trisoctahedron (TOH), and hexoctahedron (HOH). Each polyhedron is characterized by various small facets that are closely associated with its specific shape. For instance, the THH polyhedron consists of 24 (*hkl*) facets, where *h*, *k*, and *l* are integers and follow the condition $h > k > l = 0$. Similarly, the TPH polyhedron possesses 24 (*hkl*) facets with the condition $h > k = l > 0$. The TOH polyhedron has 24 (*hkl*) facets satisfying the condition $h = k > l > 0$, and the HOH polyhedron is composed of 48 (*hkl*) facets wherein $h > k > l > 0$[29]. Low-index facets, such as Ag (100), (111), (110) and Pt (111) facets, are flat surfaces at the atomic level, with densely packed surface atoms [Figure 2B]. While high-index facets, such as Ag (211), Pt (311) and (211), have rough surfaces with atomic steps. They often possess high surface energies and, thus, are more active for chemical reactions[30,31].

Understanding the growth behavior is the prerequisite for regulating the crystal facets. The crystal shape is determined by the growth rates of its facets. According to the crystal growth law[32], facets with slower growth rates occupy a larger fraction of the crystal surface than those with faster growth rates. This is illustrated in Figure 2C, where the dihedral angles between facets M and N are constant throughout the growth process, as dictated by the law of conservation of crystal plane angles. If facet M grows slower than facet N, then facet N will gradually shrink or vanish as the crystal grows, leaving facet M as the dominant surface. Conversely, if facet M grows faster than facet N, then facet N will become the dominant surface. Therefore, regulating the growth rates of crystal facets is crucial for exposing specific surfaces.

High-index facets are highly reactive and challenging to stabilize due to their thermodynamic instability. The synthetic methods that have been developed encompass wet chemistry, electrochemistry, and solid-state chemistry synthesis.

Currently, most high-index facet nanocrystals are synthesized using the wet chemistry method, which has the advantage of easy large-scale synthesis. Numerous studies have incorporated surfactants, polymers, capping agents, small molecules, ions, *etc.*, into the synthesis process. These additives could adsorb onto specific crystal facets and slow the growth rate (adsorption-mediated route), enabling the synthesis of nanocrystals with various crystal facet exposures. For instance, Yang *et al.* synthesized cyclic penta-twinned Rh icosahedral nanocrystals using a one-pot hydrothermal method in the presence of a capping agent [Figure 3A][33]. They found that, in addition to varying the concentration or type of capping agent, the solvent could affect the adsorption capacity of the surfactant on the Rh crystal surface, leading to a change in surface free energy and, thus, permitting the formation of Rh cyclic penta-twinned nanostructures. Moreover, it is possible to regulate the growth kinetics (kinetically controlled route) by coordinating with reactant precursors to expose different crystal facets. According to crystal growth theory, nanocrystal growth involves the diffusion of precursors from the solution to the surface, the deposition of new atoms, and the migration of newly deposited atoms on the surface. Corners and edges have higher solution transfer rates due to their small radius of curvature. When the deposition rate exceeds the surface diffusion rate, the growth is kinetically controlled, and concave nanocrystals typically form due to overgrowth at the corners and edges. For example, Liang *et al.* synthesized Fe_2O_3 concave nanocubes with (1344) and (1238) crystal facets [Figure 3B][34]. In kinetically controlled synthesis, the reaction rate can be varied by the reductant and precursor concentration, the injection rate, the number of crystalline species, and the reaction temperature. The nanocrystal surface structure can also be regulated by adjusting the supersaturation degree; the higher the supersaturation degree of the growth unit, the higher the nanocrystal surface energy. The supersaturation degree can be controlled by the reduction rate; the faster the reduction rate, the greater the degree of supersaturation of the growth unit and the more open the surface of the resulting nanocrystals. Through this method, convex polyhedral nanocrystals, including Cu_2O [Figure 3C][35] and others, can be obtained.

However, the morphology control agents (typically organic molecules) are challenging to remove during the wet chemistry synthesis process, often impeding the catalytic activity. Consequently, the synthesis of high-index facet nanocrystals with clean surfaces primarily follows the electrochemical method. This technique, however, also has limitations in scaling up and in the universal preparation of nanocrystals. Electrochemical synthesis is predominantly based on the square-wave potential (SWP) method, which induces periodic oxygen adsorption and desorption. Over the past decade, various metal nanocrystals with different high-index facets and compositions have been synthesized using electrochemical SWP methods. For example, Hu *et al.* prepared trapezohedral Pt nanocrystals surrounded by (311) high-index facets on a glassy carbon electrode using the electrochemical SWP method [TPH Pt-(311)][36]. The surface structures of the prepared

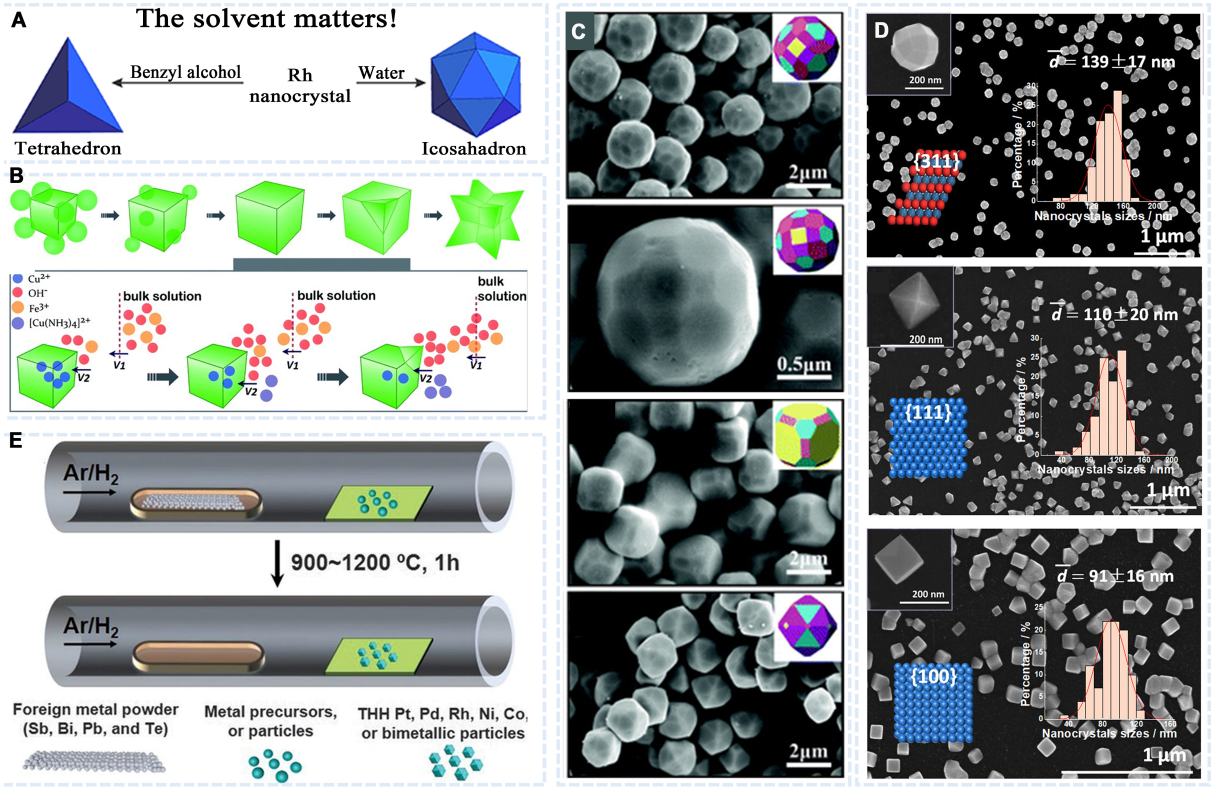

Figure 3. (A) Diagram of synthesizing Rh nanocrystals of different shapes in different solvents. Reproduced with permission[33]. Copyright 2018, Springer Nature; (B) Schematic diagram of the kinetically controlled overgrowth (when V_2 is much larger than V_1) of concave nanocubes evolved from pseudo-nanocubes. Reproduced with permission[34]. Copyright 2014, Royal Society of Chemistry; (C) SEM images of Cu_2O polyhedra synthesized with different concentrations of NaOH. Reproduced with permission[35]. Copyright 2012, The Royal Society of Chemistry; (D) SEM images of Pt (311), (111) and (100). The inset presents size histogram and atomic model of the facet. Reproduced with permission[36]. Copyright 2023, OAE Publishing Inc; (E) Scheme for synthesizing THH particles. Reproduced with permission[37]. Copyright 2019, American Association for the Advancement of Science. SEM: Scanning electron microscopy; THH: tetrahexahedron.

Pt nanocrystals were investigated by cyclic voltammetry scanning. The oxygen adsorption currents in the oxygen species adsorption and desorption regions were significantly larger for TPH Pt-(311) than for Pt (111) and Pt (100) [Figure 3D]. This is primarily due to the preferential adsorption of oxygen atoms onto the step atoms with lower coordination numbers, suggesting that the TPH Pt-(311) surface has a higher density of step atoms.

Foreign metals can alter the surface energy of nanocrystals. Therefore, the deposition of foreign metals on metal nanocrystals by underpotential deposition (UPD) can obstruct specific crystal facets (UPD-mediated route), enabling the nanocrystal synthesis with different crystal facet exposures. Huang *et al.* prepared THH nanocrystals of Pt, Pd, Rh, Ni, Co, and bimetallic particles by solid-state chemistry, with sizes ranging from 10 to 500 nm [Figure 3E][37]. The solid metal precursors were heated in a tube furnace, where the nanoparticle growth was influenced by an atmosphere containing foreign metals (Sb, Bi, Pb, and Te). In this process, an alloy is initially formed and then de-alloyed by evaporating the heterogeneous metals at higher temperatures, forming a THH nanocrystal primarily surrounded by (210) facets.

In summary, synthesizing different crystal facets and exposing various step atoms can not only change the intrinsic activity of the catalyst, accelerate the electron transfer and optimize the adsorption of

intermediates, but also change the active site, which can greatly optimize the performance if there are more intermediate stations of electron transfer with the reactant intermediates. Similarly, in the field of electrocatalytic NtrRR, we will discuss how the crystal facets would affect the NtrRR performance below.

ELECTROCATALYSTS WITH SPECIFIC LOW-INDEX FACETS FOR THE NTRRR

Noble metal electrocatalysts

Noble metals have been identified as highly active electrocatalysts for NtrRR. They crystallize in a cubic crystal system, and the regulation of crystal facets is relatively easy. Many researchers have investigated the influence of crystal facets on the selectivity and activity of NtrRR, aiming to further optimize the catalytic performance. Han *et al.* synthesized Pd cubes, octahedra, and rhombic dodecahedra with exposed (100), (111), and (110) facets using a simple seed-mediated method [Figure 4A][38]. In neutral conditions, Pd (111), (110), and (100) crystal facets were tested for NH_3 yield, Faraday efficiency, and selectivity. The Pd (111) yielded 0.5485 mmol·h^{-1}·cm^{-2} NH_3, with a Faraday efficiency of 79.91% and an NH_3 selectivity of 77.26%, along with excellent durability for 20 h of electrolysis. Density functional theory (DFT) calculations indicated that NO_3^- tends to adsorb more on the Pd (111) surface, exhibiting lower HER activity, which benefits the NtrRR. Since the NtrRR involves various intermediates, and different crystal facets exhibit varying interaction behavior with these intermediates, the performance of the electrocatalysts might be further boosted by combining diverse facets. For instance, Lim *et al.* synthesize Pd nanoparticles with controlled crystal facets, including Pd nanocubes with exposed (100) facets, octahedra with (111) facets, cubic octahedra with (100) and (111) facets, concave nanocubes with (100), and high-index (hk0) facets [Figure 4B][39]. Electrochemical measurements revealed that the Pd (111) facet facilitated the reduction of NO_3^- to NO_2^-, while the Pd (100) facet aided the conversion of NO_2^- to NH_3. DFT calculations further indicated that the adsorption and desorption rates of NO_3^- on the Pd (111) surface are relatively fast, while the energy barrier for NO_2^- desorption and dissociation on the Pd (100) surface is low. This explains the synergy between the exposed (111) and (100) facets largely enhances the NtrRR performance. As a result, the Pd cubic octahedra composed of these two facets delivered a high NH_3 yield of 307 μg·h^{-1}·mg^{-1}.

In a similar vein, Guo *et al.* employed DFT calculations to predict the NtrRR energetics on the Rh (111) (110) and (100) facets [Figure 4C] by investigating the surface adsorption of five major species (NO_2, NO, N_2O, N_2, and NH_3) involved in NtrRR[40]. The findings suggest that the exposed facets of Ru substantially influence the energetics of the NRR (NtrRR). Among the different facets studied, Rh (100) showed the highest level of activity for ammonia production. Furthermore, the optimal potential range for achieving efficient NtrRR on Rh (100) was identified to be between 0.15-0.09 V *vs.* RHE. They further conducted the experiments to verify the calculation results, and a peak NH_3 yield of 34.4 μg·h^{-1}·cm^{-2} was achieved. However, the Faraday efficiency turned out to be unexpectedly low (20.8%). Interestingly, Liu *et al.* demonstrated Rh nanoflowers with the (111) facet as the main exposed surface exhibit decent NtrRR performance with a high Faraday efficiency of 95% at the potential of 0.2 V *vs.* RHE [Figure 4D][41]. In addition, the required overpotential of the Rh nanoflowers was also much lower than most catalysts reported so far. The contradictory results from these two studies indicate that the role of crystal facets might be more complex and require further investigation. X-ray absorption spectroscopy analysis suggested that Rh nanoflowers have abundant low coordination Rh atoms. DFT calculations further revealed that these atoms can enhance the adsorption of NO_3^- and better stabilize reaction intermediates, therefore resulting in superior NtrRR performance.

Among all noble metals, Pt is perhaps the most extensively studied electrocatalyst for the NtrRR because of its strong electrocatalytic performance and excellent reduction effectiveness. Katsounaros *et al.* analyzed the NtrRR energetics on Pt (111) and (100) in an acidic nitrate electrolyte[42]. They discovered that $^*NO$ is a key

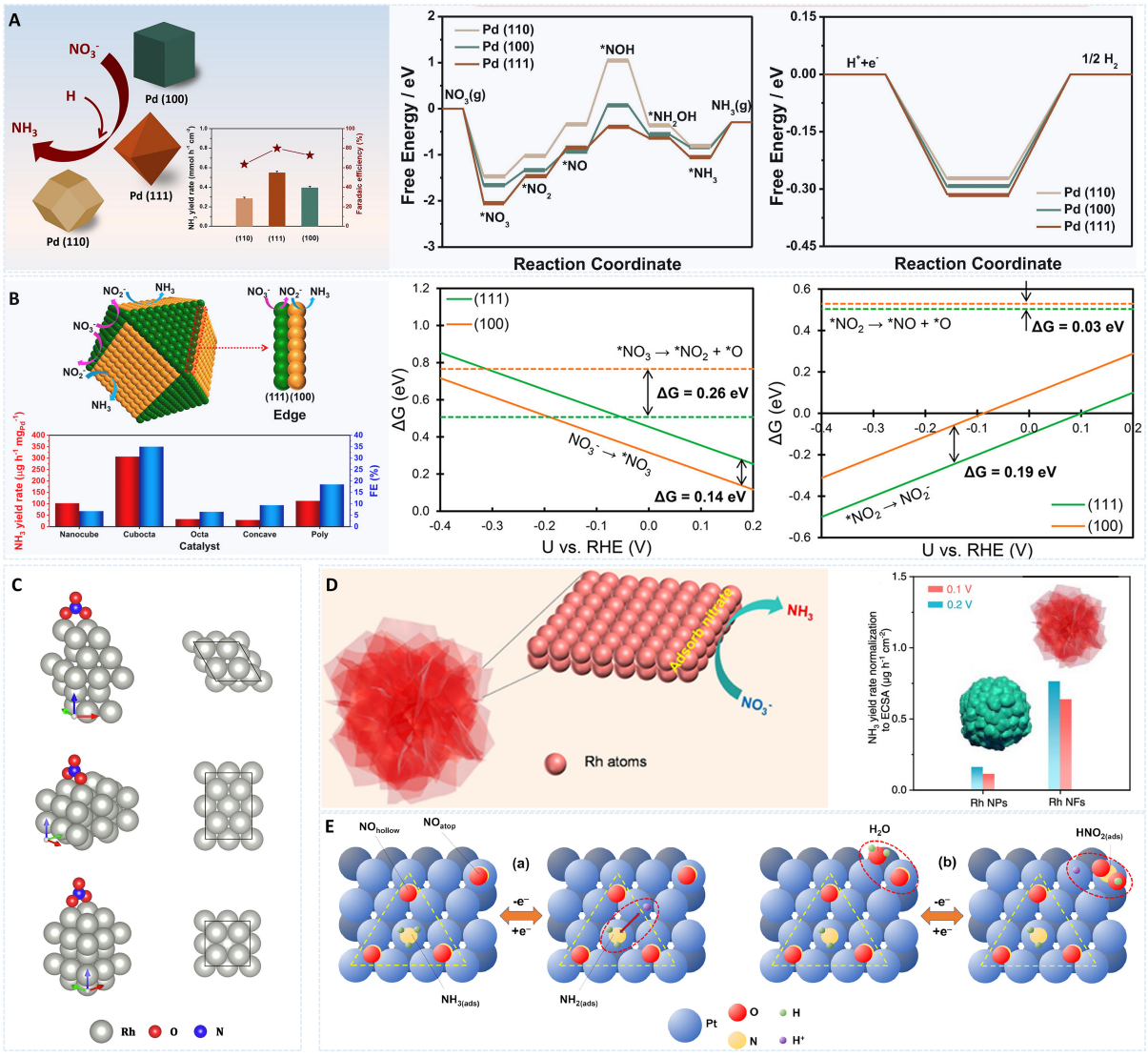

Figure 4. Noble metal electrocatalysts with low-index facets for the NtrRR. (A) NH_3 yield rates and Faraday efficiencies of Pd (111), (110), and (100) facets (left panel). Free energy diagram for NtrRR (middle) and the reaction energies of H_2 formation (right) over Pd (111), (110), and (100) facets. Reproduced with permission[38]. Copyright 2021, Elsevier; (B) NH_3 yield rates and Faraday efficiencies of Pd catalysts with different shapes (left panel). Adsorption energy of NO_3^- (middle) or NO_2^- (right) at pH = 0 and the activation barrier for converting $^*NO_3$ to $^*NO_2$ and $^*NO_2$ to $^*NO$. Reproduced with permission[39]. Copyright 2021, American Chemical Society; (C) Surface configurations of nitrate adsorption on Rh (111), (110), and (100) facets. Reproduced with permission[40]. Copyright 2021, Elsevier; (D) Diagrammatic representation of the low coordination Rh atoms (left panel) and the NH_3 yield rate of Rh nanoparticles and nanoflowers (right). Reproduced with permission[41]. Copyright 2023, American Chemical Society; (E) Schematic illustration of the reversible redox-transitions on Pt surface. Reproduced with permission[43]. Copyright 2023, Elsevier.

intermediate and could poison the Pt surface. They further demonstrated that only Pt (111) could achieve the complete conversion of NO_3^- to NH_3 in a narrow potential window. This behavior, however, could significantly differ in alkaline electrolytes. Molodkina *et al.* demonstrated that among all Pt facets, the Pt (100) facet exhibits the highest activity in the reduction of NO_3^- and NO. In contrast, the Pt (111) facet shows structural sensitivity in the reduction of NO_3^- and NO, with incomplete reduction of NO on Pt (111)[43]. They found that $^*NO$ occupies two different types of sites on the Pt (111) surface: atop and 3-fold hollow. $^*NO$ adsorbed on atop surface sites is reduced to form $^*NH_3$ and stabilized by adsorption on hollow sites. The produced ammonia does not detach but creates co-adsorption compounds with adjacent NO

molecules bound to hollow sites, which are supported by dipole-dipole interactions and hydrogen bonding. Upon affecting the reduction degree of the adsorbed layer by the $^*NO$, the $^*NO/^*NH_3$ complexes start to decompose. Due to this, hydrogen adatoms formed in the respective range of potentials cause the adsorption of NH_3 on the surface to weaken. As long as no further reduction occurs and the electrode remains within the potential range in which hollow-bound NO molecules are not reduced, co-adsorption complexes are expected to remain stable. In these circumstances, there is a transition from hydrofluoric acid to hydrogen chloride at potentials around 0.6 V. Although the hydrogen bonds may become less strong due to the degradation of the hydrofluoric acid, the strong dipole-dipole interactions stabilize the complex. Relativistic 1.1 V conditions result in reversible oxidation of atop-bound NO species to nitrite species (HNO_2). Conversely, hollow-bound NO species do not oxidize when co-adsorption is formed with $^*NH_2$. As a result, no NO to HNO_2 redox transition occurs [Figure 4E].

Non-noble metal electrocatalysts

While noble metal electrocatalysts show good NtrRR performance, their high cost limits the large-scale application. Considerable endeavors have thus been dedicated to investigating alternative catalysts based on non-noble metals. Among them, Cu-based materials are the most widely studied. The relatively large hydrogen adsorption free energy (ΔG_H) on these materials can inhibit the competitive HER. Moreover, their d-orbital energy levels are similar to the LUMO π^* of NO_3^-, making them good electrocatalysts towards the NtrRR. Hu *et al.* used DFT to calculate the pathway of NtrRR on Cu (111), (100), and (110) facets at different pH values [Figure 5A][44]. There was a significant pH effect on the catalytic hydrogenation and deoxygenation processes. Further study showed that pH was also a factor for rate control steps and overpotential. In addition, pH value changes can also affect the competition between HER and NtrRR. Through studying the NH_3 generation from NtrRR and HER on different crystal facets, it was found that Cu (100) and (111) facets contribute the most to the NtrRR, while Cu (110) contributes the least. In particular, in near-neutral and alkaline environments, Cu (111) is most effective, whereas Cu (100) is most effective in strongly acidic environments. According to the author, the local coordination environment and the electronic states of surface atoms are responsible for the different NtrRR levels towards NH_3 production on the Cu surface. Due to the stereospecificity of Cu-Cu pairs, strong $^*NOH$ adsorption and weak $^*NH_3$ adsorption were achieved on Cu (111) and (100), thereby promoting the NtrRR. To further improve the catalytic performance of Cu-based materials with a single crystal facet, Fu *et al.* developed Cu nanosheets derived *in situ* from CuO nanosheets for NtrRR [Figure 5B][45]. *In situ* electrochemical spectroscopy determined which phases were catalytically active in the prepared CuO nanosheets. The Cu K-edge X-ray absorption near edge structure (XANES) spectra of the CuO nanosheet electrocatalyst prepared at open circuit potential (OCP) were similar to the reference CuO, indicating their resemblance in absorption edges. However, applying NtrRR current caused a shift in the spectra of the CuO nanosheet towards the reference Cu foil, suggesting an electrochemical reduction of the CuO nanosheets to metallic Cu *in situ*. The outstanding performance of the electrocatalyst was ascribed to the synergistic effect between the Cu (100) and (111) facets, as confirmed by electrochemical tests and DFT calculations. The presence of Cu (100) facilitated the generation of NO_2^-, which was subsequently hydrogenated on the Cu (111) facet, promoting the hydrogenation of $^*NO$ to $^*NOH$ through a relay catalysis mechanism. The Cu nanosheet catalyst has a current density of 665 mA·cm^{-2} at -0.59 V *vs.* RHE, an NH_3 yield of 1.41 mmol·h^{-1}·cm^{-2}, a Faraday efficiency of 88%, and a high stability for 700 h at 365 mA·cm^{-2}. In addition, Hu *et al.* developed an electrocatalyst synthesis strategy based on *in situ* electrochemical reduction of copper oxide nanoribbons under NtrRR conditions [Figure 5C][46], which effectively exposed the Cu (100) surface with abundant surface defects that significantly promoted the generation of NtrRR and effectively suppressed HER. Impressively, in alkaline media, the yield of NH_3 catalyzed by defective Cu (100) surface is 2.3 times higher than that generated through the Haber Bosch process. They demonstrated using $^*N$ as a capping agent to regulate the exposed surface while carrying out the reduction process. The upward shift of the d-band center of copper, brought

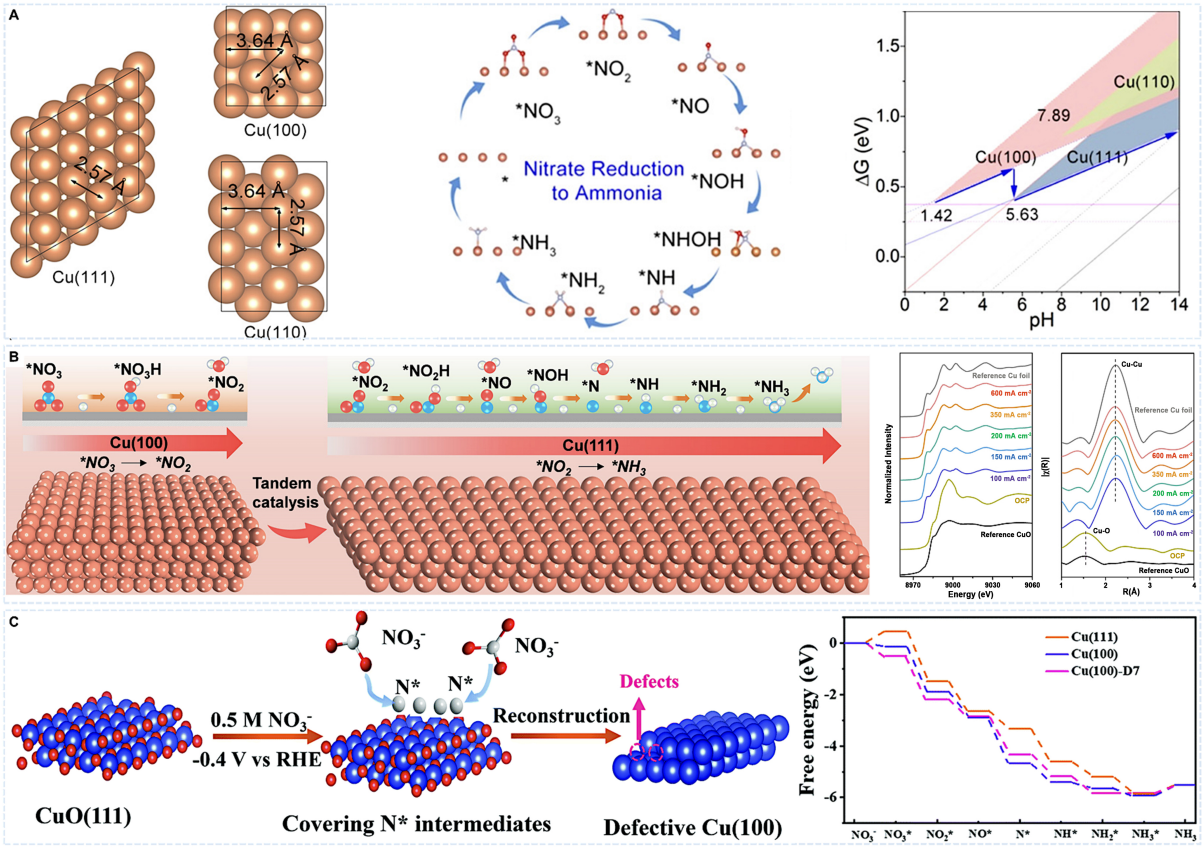

Figure 5. Cu-based electrocatalysts with low-index facets for the NtrRR. (A) Surface structures of Cu (111), (100), and (110) (left panel), NtrRR mechanism on Cu (111) (middle), and the ΔG for different facets at different pH (right). Reproduced with permission[44]. Copyright 2021, American Chemical Society; (B) Tandem interaction of Cu (100) and (111) facets (left panel). *In situ* Cu K-edge XANES and EXAFS spectra of CuO nanosheets under various conditions (right). Reproduced with permission[45]. Copyright 2023, Wiley Online Library; (C) Graphical depiction of NtrRR intermediate (*N) adsorption on CuO (111) nanobelts (left panel) and the free energy diagrams illustrating the reaction pathways for NH_3 formation through NtrRR (right). Reproduced with permission[46]. Copyright 2021, Wiley Online Library. XANES: X-ray absorption near edge structure; EXAFS: extended X-ray absorption fine structure.

about by the synergistic effect of Cu (100) crystal facet and defects, holds the key to attaining outstanding performance.

Furthermore, Zhong *et al.* synthesized Cu_2O with exposed (100), (111), and mixed (100) and (111) facets [Figure 6A][47] and coherently studied the effect of surface oxygen species on the NtrRR elementary reaction. They found that the Cu_2O surface with the exposed (111) crystal facet has the highest density of oxygen vacancies and hydroxyl groups. Oxygen vacancies would facilitate the adsorption of reactants and intermediates, while hydroxyl groups inhibit the HER, thereby promoting the hydrogenation process of NtrRR. As a result, Cu_2O with exposed (111) facets demonstrated the most superior NtrRR efficiency, with a high NH_3 selectivity of 97.59%. While the reaction intermediates detected in Fourier transform infrared spectroscopy (FT-IR) were alike on the Cu_2O (100) and (111) facets, the adsorption of reaction intermediates on the (111) facet was significantly stronger than on the (100) facet for a specified electrolysis duration. In addition, a distinct N-H peak was noted during a briefer electrolysis period for the Cu_2O (111) compared to the Cu_2O (100), which corroborates the elevated ammonia yield and selectivity observed on the Cu_2O (111).

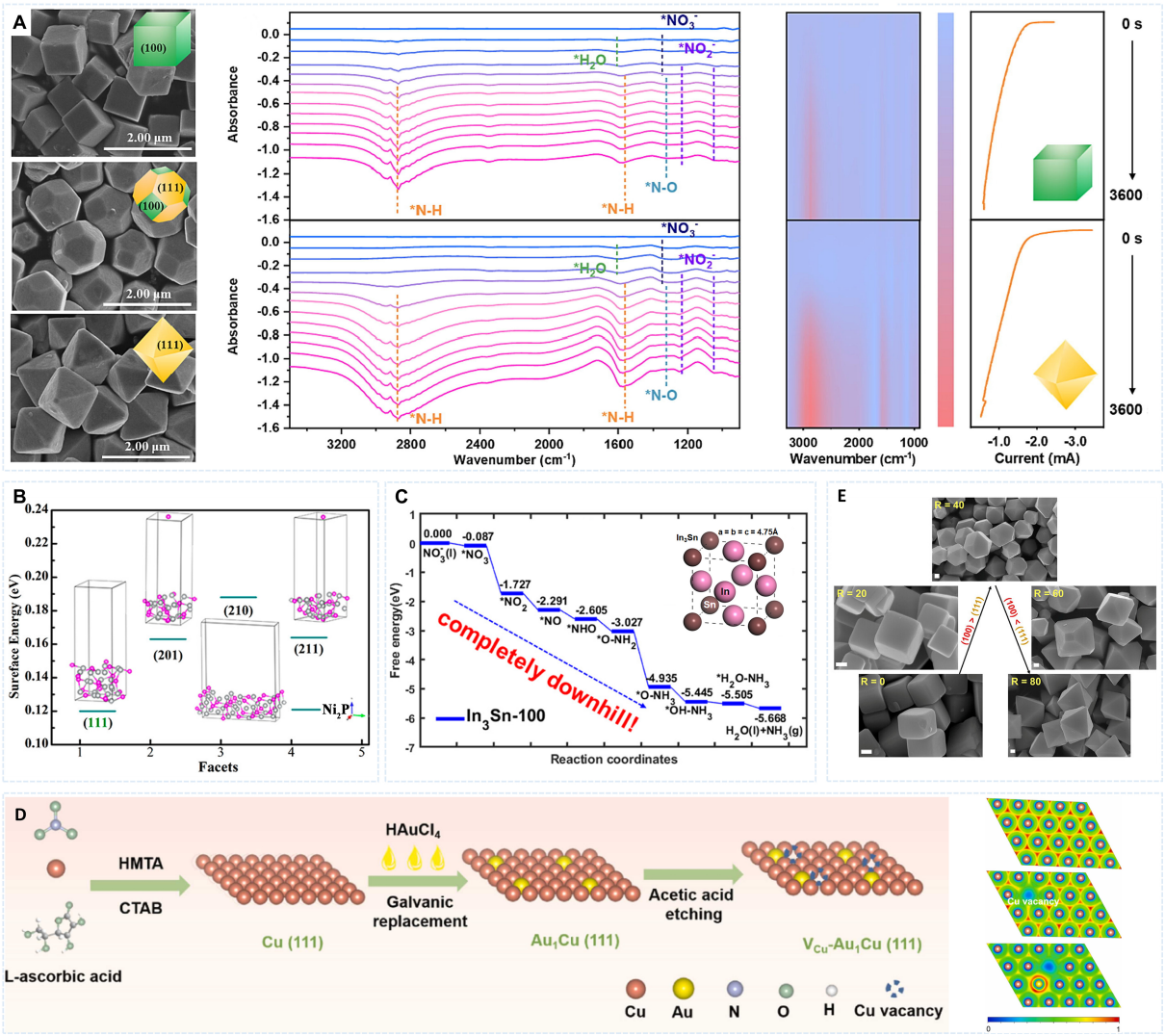

Figure 6. Non-noble metal electrocatalysts with low-index facets for the NtrRR. (A) SEM images of the Cu_2O with specific exposed facet (left panel) and the time-dependent *in-situ* FT-IR spectra: Cu_2O (100) and (111) electrocatalyst at -1.2 V *vs.* Ag/AgCl in nitrate solution (middle and right). Reproduced with permission[47]. Copyright 2022, Elsevier; (B) Surface energy diagrams of Ni_2P with different orientations. Reproduced with permission[48]. Copyright 2021, American Chemical Society; (C) The NtrRR free energy diagram of In_3Sn (100). Reproduced with permission[17]. Copyright 2023, American Chemical Society; (D) Illustrative diagram of the V_{Cu}-Au_1Cu SAAs synthetic procedure (left panel) and differential charge densities of the Cu NSs (top), V-Cu NSs (middle), and V_{Cu}-Au_1Cu SAAs (bottom). Blue: charge depletion, red: charge accumulation (right). Reproduced with permission[50]. Copyright 2022, Elsevier; (E) SEM images: Au/Cu SAAs. Reproduced with permission[51]. Copyright 2023, American Chemical Society. SEM: Scanning electron microscope; FT-IR: Fourier transform infrared spectroscopy; SAAs: single-atom alloys.

In addition to Cu, other transition metals have also been investigated. As a demonstration, Yao *et al.* synthesized Ni_2P with the exposed (111) facet on a Ni foam as a self-supported electrocatalyst for the NtrRR, which achieved an NH_3 yield of up to 0.056 mmol·h^{-1}·mg^{-1} and a Faraday efficiency of up to 99.23%[48]. They found that the Ni_2P (111) can promote the water dissociation and generate active hydrogen atom $^*H$, which then induced the $^*H$-mediated reaction pathway and thus achieved a high NH_3 selectivity. DFT calculations further revealed that among Ni_2P (111), (201), (210), and (211), the (111) facet possesses the minimal surface energy and is stable in a real environment [Figure 6B], and NO_3^- is more likely to be adsorbed on the Ni_2P (111 facet; the hydrogenation of $^*NO$ to NH_3 is thermodynamically favorable ($\Delta G < 0$). It is noted that

almost all of the reported non-noble NtrRR catalysts are based on transition metals. However, Yin *et al.* indicated that, through DFT calculations, In-based transition metal-free compounds, especially In_3Sn[17], could be excellent NtrRR electrocatalysts. They identified a new reaction pathway on In_3Sn (100) surface, along which the changes in free energy are always negative, indicating the thermodynamically feasible of the pathway [Figure 6C]. In addition, it was found that proton adsorption on the In_3Sn (100) surface was very weak, substantially inhibiting parasitic HER. Crawford *et al.* experimentally confirmed that InSn in a Ga-based liquid metal electrocatalyst exhibits decent NtrRR performance with an NH_3 yield of 2,335 $\mu g \cdot h^{-1} \cdot cm^{-2}$ with a Faraday efficiency of 100%, and the InSn was identified as the active sites[49].

Composite electrocatalysts with noble and non-noble metals

It should be noted that in most cases, the NtrRR performance of non-noble electrocatalysts is still inferior to that of noble metals. On the other hand, noble metal electrocatalysts suffer from high cost. Therefore, researchers are exploring the potential of composite electrocatalysts with noble and non-noble metals, aiming to achieve an optimal balance of both the activity and cost.

Zhang *et al.* designed an Au_1Cu (111) single-atom alloy (SAA) with Cu vacancies on the surface (V_{Cu} Au_1Cu SAA) [Figure 6D][50], which exhibited an NH_3 Faraday efficiency of up to 98.7% and an NH_3 yield of 555 $\mu g \cdot h^{-1} \cdot cm^{-2}$ at -0.2 V *vs.* RHE. Characterization results indicated that in V_{Cu} Au_1Cu SAA, electron migration from Cu to Au atoms generates electron-deficient Cu active sites. This promoted the generation of active hydrogen species $^*H$ and facilitated NO_3^- reduction. According to theoretical calculations, the Cu sites with specific crystal facets and defects exhibit dual functionality. These facets not only aid in the activation of water to generate $^*H$ but also decrease the energy barrier for the desorption of $^*NH_3$ from the catalyst surface. In another study, Yin *et al.* successfully deposited Au atoms on Cu nanoparticles with (100) surface exposure [Au/Cu (100) SAAs] [Figure 6E][51]. Their performance for NtrRR surpassed that of Cu (100) and Au/Cu (111) SAAs. AuCu (100) SAAs effectively inhibited the generation of N-N coupled N_2O or N_2. They claimed that Au single atoms (SAs) significantly reduce the adsorption energy of NO_3^- on Cu (100), and the Au–Cu bonds form in NtrRR contribute to the reduction of NO_2 to NO intermediates. This resulted in a high NH_3 Faraday efficiency of 99.69% at -0.80 V *vs.* RHE.

ELECTROCATALYSTS WITH SPECIFIC HIGH-INDEX FACETS FOR THE NTRRR

High-index facets, in contrast to low-index facets, have a higher concentration of low coordination atoms, such as steps and twist sites. Consequently, these high-index facets often demonstrate enhanced electrocatalytic performance. The application of crystal facets as model catalysts in fundamental studies has shown that high-index facet-centered cubic (FCC) metals, such as Pt, Pd, Ir, Au, Ag, Cu, and Ni, exhibit remarkable catalytic activity for a wide range of chemical reactions, including the NtrRR. For example, Chen *et al.* synthesized tetrahedral Cu nanocrystals with exposed (520) high-index [THH Cu(520)] facets using an electrochemical square wave potential method without additional capping agents [Figure 7A][52]. The catalyst exhibited excellent NtrRR performance. In a neutral solution, at a potential of -0.90 V *vs.* RHE, the Faraday efficiency was as high as 98.3%, and the NH_3 yield was as high as 9.13 $mmol \cdot h^{-1} \cdot cm^{-2}$. This performance significantly surpassed that of Cu nanocrystals with exposed (100) and (111) low-index facets. By adjusting the adsorption strength of intermediates through alloying, the electrocatalytic activity can be further improved. Liu *et al.* synthesized concave octahedral TOH Au-Pd alloy nanocrystals with exposed (331) high-index facets using the electrochemical double-step potential method [Figure 7B][53]. The results indicated that due to the low coordination number of high-index facets and the electronic interactions of Au-Pd alloys, the concave TOH Au-Pd alloy nanoparticles exhibit excellent NtrRR activity and selectivity compared with Au (311) and (111) facets [Figure 7C]. Remarkably, under ambient conditions, the highest NH_3 yield of 4,591.71 $\mu g \cdot h^{-1} \cdot mg_{cat}^{-1}$ and the Faraday efficiency was 62% was achieved at a potential of -1.15 V

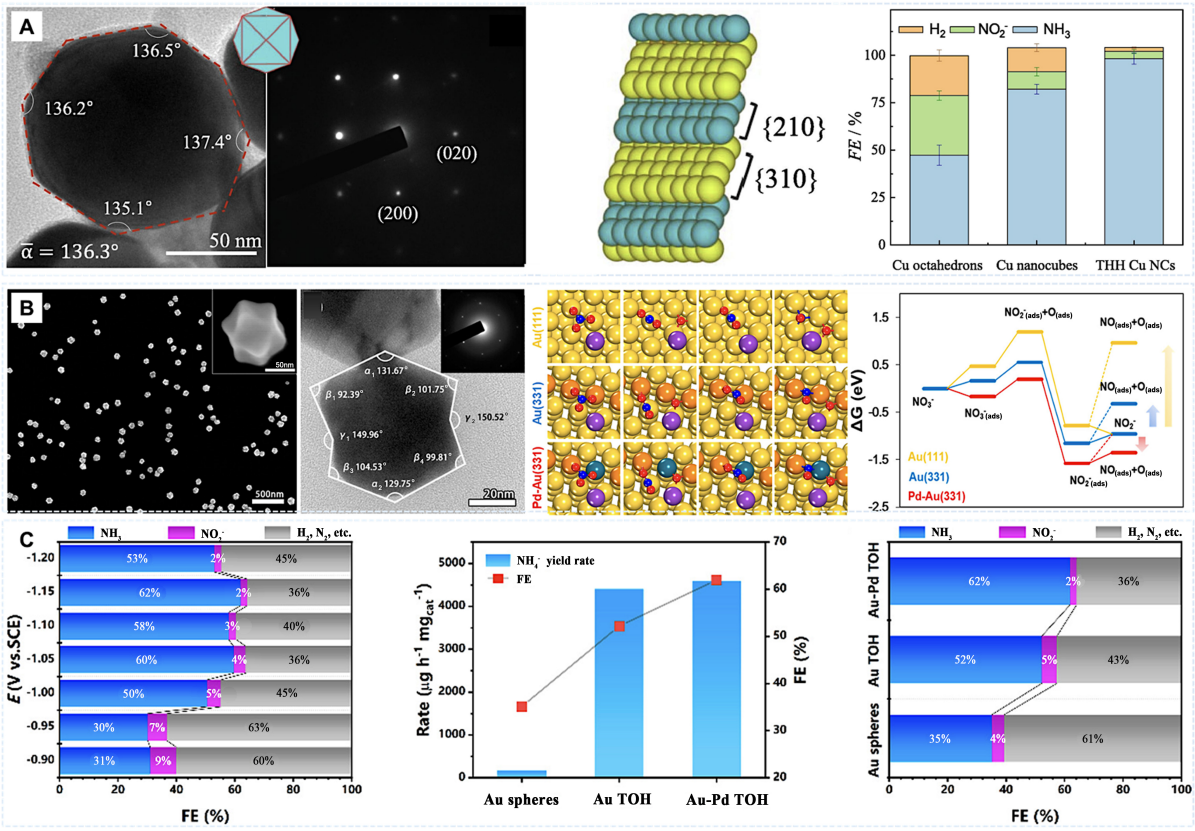

Figure 7. Electrocatalysts with high-index facets for the NtrRR. (A) TEM image, SAED pattern of a THH Cu NC (left panel), atomic model of (520) facet (middle), and Faraday efficiencies of various Cu catalysts (right). Reproduced with permission[52]. Copyright 2022, Elsevier; (B) SEM image, TEM image, and the corresponding SAED patterns of concave TOH Au–Pd NCs (left panel), optimized structures of intermediates of $^*NO_3^-$, $^*NO_2^-$ + $^*O$, $^*NO_2^-$ and $^*NO$ + $^*O$ (middle), and free energy profiles for NtrRR on Au (111) and (331), and TOH Au–Pd NCs (right). Reproduced with permission[53]. Copyright 2023, American Chemical Society; (C) Faraday efficiencies of main products at different working potentials of TOH Au–Pd NCs (left panel), NH_3 yield rate and Faraday efficiencies of Au (111), Au (331), and TOH Au–Pd NCs (middle), and FE of main products of Au (111), Au (331), and TOH Au–Pd NCs at -1.15 V *vs* SCE (right). Reproduced with permission[53]. Copyright 2023, American Chemical Society. TEM: Transmission electron microscopy; SAED: selected area electron diffraction; THH: tetrahexahedron; NC: nanocrystals; SEM: scanning electron microscope; TOH: trisoctahedron; FE: Faraday efficiency; SCE: saturated calomel electrode.

vs. saturated calomel electrode (SCE). DFT calculations indicated that the Pd-modified Au (331) step surface endows high activity for NO_3^- adsorption and N–O bond cleavage, enhancing the activity and selectivity of NtrRR. Although high-index facets show promising NtrRR performance, their synthesis is generally much more challenging, and thus, electrocatalysts with high-index facets have considerably less been investigated for NtrRR.

CONCLUSIONS AND PERSPECTIVES

Over the past few years, significant strides have been made in exploring efficient electrocatalysts in terms of crystal facet engineering for nitrate reduction to ammonia, from low-index to high-index facets, from single metals to alloys and further more complex composites. The current review summarizes the current progress in crystal facets engineering of NtrRR electrocatalysts [Table 1].

The facet-engineered catalysts can not only provide more active and selective sites for the NtrRR by tuning the adsorption and activation energies of the reactants and intermediates but also modulate the electron

Table 1. Key performance parameters of low-index and high-index facets electrocatalysts in the NtrRR

Catalyst	Specific crystal facet	Synthetic method	Electrolyte	NH_3 faradaic efficiency	NH_3 yield rate	Authors
Pd	(111)	Wet-synthesis	0.1 M Na_2SO_4 and 0.1 M KNO_3	79.91%	2.74 $mmol·h^{-1}·mg^{-1}$	Han *et al.*[38]
Rh	(111)			95%	0.8 $\mu g·h^{-1}·cm^{-2}$	Liu *et al.*[41]
Pd	(111), (100)		0.1 M NaOH and 20 mM $NaNO_3$	35%	307 $\mu g·h^{-1}·mg^{-1}$	Lim *et al.*[39]
Cu	(100), (111)		1 M KOH and 0.2 M KNO_3	88%	1.41 $mmol·h^{-1}·cm^{-2}$	Fu *et al.*[45]
Cu_2O	(111)		0.5 M Na_2SO_4 and 100 ppm $NaNO_3$	97.59%	0.075 $mmol·mg_{cat}^{-1}·h^{-1}$	Zhong *et al.*[47]
V_{Cu} Au_1Cu SAA	Cu (111)		0.1 M KOH and 7.14 mM NO_3^-	98.7%	555 $\mu g·h^{-1}·cm^{-2}$	Zhang *et al.*[50]
Au/Cu SAAs	Cu (100)		0.5 M Na_2SO_4 and 100 ppm $NaNO_3$	99.69%	0.193 $mmol·h^{-1}·cm^{-2}$	Yin *et al.*[51]
Cu	(111), (100)		Near-neutral and alkaline strong acidic	-	-	Hu *et al.*[44]
Rh	(100)		Alkaline	20.8%	34.4 $\mu g·h^{-1}·cm^{-2}$	Guo *et al.*[40]
Cu	(100)	Electrosynthesis	1 M KOH and 0.1 M KNO_3	95.3%	650 $mmol·g_{cat}^{-1}·h^{-1}$	Hu *et al.*[46]
Cu	(520)		100 mM K_2SO_4 and 100 mM KNO_3	98.3%	9.13 $mmol·h^{-1}·cm^{-2}$	Chen *et al.*[52]
Au-Pd	Au (331)		0.5 M K_2SO_4 and 0.05 M KNO_3	61.96%	4,591.71 $\mu g·h^{-1}·mg_{cat}^{-1}$	Liu *et al.*[53]
Pt	(111)	Solid-state synthesis	Acidic	-	-	Molodkina *et al.*[43]
Ni_2P	(111)		0.5 M Na_2SO_4 and 80 $mg·L^{-1}$ $NaNO_3$	99.23%	0.056 $mmol·h^{-1}·mg^{-1}$	Yao *et al.*[48]
In_3Sn	(100)		-	-	-	Yin *et al.*[17]

SAA: Single-atom alloy.

transfer and mass transport processes. In addition, crystal facet engineering can be combined with other strategies, such as doping, alloying, heterostructuring, and defect engineering, to further improve the NtrRR performance. Despite the great progress, many challenges yet also great opportunities persist in this field.

(1) The synthesis of electrocatalysts with specific crystal facets, particularly high-index facets, is often quite challenging and requires precise control and advanced techniques. Currently, most of the reported catalysts with high-index facets crystallize in a simple cubic crystal system, while more complex compounds such as oxides have considerably less been explored. Therefore, more efficient and reliable methods for synthesizing and characterizing the facet-engineered catalysts with high quality and reproducibility need to be developed.

(2) The stability and durability of the facet-engineered catalysts are often compromised by the surface reconstruction, aggregation, and dissolution under harsh reaction conditions. Indeed, self-reconfiguration induced by potential is a frequently observed phenomenon in electrocatalysis. This is particularly true during the anodic oxidation process, which can lead to substantial alterations in the composition and structure of electrocatalysts. While catalyst reconstruction during the cathodic reduction process is relatively uncommon, studies still indicate that such a process can occur. For example, Li *et al.* discovered that the NiCu bimetallic hydroxide (NiCu-OH) catalyst rapidly converts into a composite of crystalline metallic copper (*c*-Cu) and amorphous nickel hydroxide [*a*-$Ni(OH)_2$] during the NtrRR[54]. The reconstruction not only alters the material composition but also changes the crystal facet exposed by the catalyst. It transitions from the $Cu_2(OH)_3(NO_3)$-exposed (121) facet to the Cu-exposed (111) facet. In this

case, the engineered facets might not be the real active sites, and thus, the role of crystal facets in the NtrRR electrocatalysis needs to be carefully evaluated. Real-time monitoring of the surface facet evolution is, therefore, essential to reveal the detailed electrocatalytic reaction mechanism on specific facets.

(3) NtrRR is a complex multi-step process involving various intermediates and pathways, and the reaction mechanism is still not fully understood. In this case, how the crystal facets affect the reaction mechanism requires further investigation. In addition, there is a current absence of standardized criteria for evaluating the performance of NtrRR. Various reported catalysts were tested under different conditions (e.g., the type and concentration of the supporting electrolyte, applied potential, and cumulative ammonia production time). This brings additional difficulty in comparing the activity of reported catalysts with specific exposed facets. In this regard, the reaction conditions and parameters, such as temperature, pressure, pH, electrolyte, and potential, should be optimized, while the criteria for performance evaluation should be standardized to fairly compare the performance of different reported catalysts.

(4) The NtrRR competes with the HER on most metal surfaces. Crystal facet engineering might simultaneously promote both the NtrRR and HER. Exploring specific facets with high activity and selectivity is essential for achieving a high Faraday efficiency and selectivity towards the production of NH_3.

(5) Further research, both experimental and theoretical, should be conducted to explore the relationship between the crystal facet structure and the NtrRR performance. Using *in situ* or operational characterization techniques is essential to obtain a comprehensive understanding of the dynamic structure, activity, selectivity, and stability of catalysts. These methods enable the investigation of catalytic processes and reaction mechanisms at the atomic and molecular levels. Based on these understandings, together with the big data and artificial intelligence, the discovery of high-performance NtrRR electrocatalysts with specific exposed crystal facets can be greatly facilitated.

(6) Currently, the crystal facet engineering of the electrocatalysts mainly focuses on improving the activity and stability. Further integrating the facet-engineered catalysts with other components, such as electrodes, membranes, and reactors, is also important to achieve scalable and practical applications of the NtrRR, and there could be many engineering issues. For example, determining how to expose the specific crystal facets of the catalysts during the electrode fabrication process often involves using binders and conductive additives that could block the exposed surface.

Overall, we believe that crystal facet engineering could play a significant role in enhancing the NtrRR performance of electrocatalysts. Through this review, we hope that the readers would gain better understanding of the impacts of crystal facets on the NtrRR reaction pathway, kinetics, and thermodynamics and could find useful information for designing high-performance electrocatalysts with specific exposed facets.

DECLARATIONS

Authors' contributions

Proposed the topic of this review: Liang H
Prepared the manuscript: Zhang Y
Collectively discussed and revised the manuscript: Zhang Y, Liang H

Availability of data and materials
Not applicable.

Financial support and sponsorship
This work was supported by the Fundamental Research Funds for the Central Universities of China (Grant No. 20720210010).

Conflicts of interest
Liang H is the guest editor of the Special Issue "Energy Storage and Conversion Based on Metal-Organic Frameworks", while the other author has declared that he has no conflicts of interest.

Ethical approval and consent to participate
Not applicable.

Consent for publication
Not applicable.

REFERENCES
1. Foster SL, Bakovic SIP, Duda RD, et al. Catalysts for nitrogen reduction to ammonia. *Nat Catal* 2018;1:490-500. DOI
2. Kyriakou V, Garagounis I, Vourros A, Vasileiou E, Stoukides M. An electrochemical Haber-Bosch process. *Joule* 2020;4:142-58. DOI
3. Chang F, Gao W, Guo J, Chen P. Emerging materials and methods toward ammonia-based energy storage and conversion. *Adv Mater* 2021;33:e2005721. DOI PubMed
4. Valera-Medina A, Xiao H, Owen-Jones M, David W, Bowen P. Ammonia for power. *Prog Energ Combust* 2018;69:63-102. DOI
5. Soloveichik G. Electrochemical synthesis of ammonia as a potential alternative to the Haber-Bosch process. *Nat Catal* 2019;2:377-80. DOI
6. Smith C, Hill AK, Torrente-murciano L. Current and future role of Haber-Bosch ammonia in a carbon-free energy landscape. *Energy Environ Sci* 2020;13:331-44. DOI
7. Zhu W, Yao F, Wu Q, et al. Weakened d–p orbital hybridization in *in situ* reconstructed Ru/β-$Co(OH)_2$ heterointerfaces for accelerated ammonia electrosynthesis from nitrates. *Energy Environ Sci* 2023;16:2483-93. DOI
8. Ren Y, Yu C, Tan X, et al. Strategies to activate inert nitrogen molecules for efficient ammonia electrosynthesis: current status, challenges, and perspectives. *Energy Environ Sci* 2022;15:2776-805. DOI
9. Macfarlane DR, Cherepanov PV, Choi J, et al. A roadmap to the ammonia economy. *Joule* 2020;4:1186-205. DOI
10. Zhang F, Luo J, Chen J, et al. Interfacial assembly of nanocrystals on nanofibers with strong interaction for electrocatalytic nitrate reduction. *Angew Chem Int Ed Engl* 2023;62:e202310383. DOI
11. Wang J, Feng T, Chen J, et al. Electrocatalytic nitrate/nitrite reduction to ammonia synthesis using metal nanocatalysts and bio-inspired metalloenzymes. *Nano Energy* 2021;86:106088. DOI
12. Wu Z, Song Y, Liu Y, Luo W, Li W, Yang J. Electrocatalytic nitrate reduction: selectivity at the crossroads between ammonia and nitrogen. *Chem Catal* 2023;3:100786. DOI
13. Zhu W, Zhang X, Yao F, et al. A hydrazine-nitrate flow battery catalyzed by a bimetallic RuCo precatalyst for wastewater purification along with simultaneous generation of ammonia and electricity. *Angew Chem Int Ed Engl* 2023;62:e202300390. DOI
14. Wang Z, Liu S, Zhao X, et al. Interfacial defect engineering triggered by single atom doping for highly efficient electrocatalytic nitrate reduction to ammonia. *ACS Mater Lett* 2023;5:1018-26. DOI
15. Sun N, Guo Y, Luo L, Cai X, Shen S, Zhang J. Facile synthesis of CuCo-CoO composite electrocatalyst for nitrate reduction to ammonia with high activity, selectivity and stability. *Appl Surf Sci* 2023;624:157118. DOI
16. Bai Z, Li X, Ding L, Qu Y, Chang X. Artificial Cu-Ni catalyst towards highly efficient nitrate-to-ammonia conversion. *Sci China Mater* 2023;66:2329-38. DOI
17. Yin H, Mao X, Bell S, Golberg D, Du A. Transition-metal-free, pure p-block alloy electrocatalysts for the highly efficient nitrate reduction to ammonia. *Chem Mater* 2023;35:2884-91. DOI
18. Zhang Z, Liu Y, Su X, et al. Electro-triggered Joule heating method to synthesize single-phase CuNi nano-alloy catalyst for efficient electrocatalytic nitrate reduction toward ammonia. *Nano Res* 2023;16:6632-41. DOI

19. Xiao C, Lu B, Xue P, et al. High-index-facet- and high-surface-energy nanocrystals of metals and metal oxides as highly efficient catalysts. *Joule* 2020;4:2562-98. DOI
20. Li Y, Li M, Li S, Liu Y, Chen J, Wang Y. A review of energy and environment electrocatalysis based on high-index faceted nanocrystals. *Rare Met* 2021;40:3406-41. DOI
21. Feng S, Li D, Dong H, et al. Tailoring the Mo-N/Mo-O configuration in MoO_2/Mo_2N heterostructure for ampere-level current density hydrogen production. *Appl Catal B Environ* 2024;342:123451. DOI
22. de Groot M, Koper M. The influence of nitrate concentration and acidity on the electrocatalytic reduction of nitrate on platinum. *J Electroanal Chem* 2004;562:81-94. DOI
23. Xu B, Li D, Zhao Q, Feng S, Peng X, Chu PK. Electrochemical reduction of nitrate to ammonia using non-precious metal-based catalysts. *Coord Chem Rev* 2024;502:215609. DOI
24. Gao J, Jiang B, Ni C, Qi Y, Bi X. Enhanced reduction of nitrate by noble metal-free electrocatalysis on P doped three-dimensional Co_3O_4 cathode: mechanism exploration from both experimental and DFT studies. *Chem Eng J* 2020;382:123034. DOI
25. Tong W, Huang B, Wang P, Shao Q, Huang X. Exposed facet-controlled N_2 electroreduction on distinct Pt_3Fe nanostructures of nanocubes, nanorods and nanowires. *Natl Sci Rev* 2021;8:nwaa088. DOI PubMed PMC
26. Tan L, Yang N, Huang X, et al. Synthesis of ammonia *via* electrochemical nitrogen reduction on high-index faceted Au nanoparticles with a high faradaic efficiency. *Chem Commun* 2019;55:14482-5. DOI
27. Bao D, Zhang Q, Meng FL, et al. Electrochemical reduction of N_2 under ambient conditions for artificial N_2 fixation and renewable energy storage using N_2/NH_3 cycle. *Adv Mater* 2017;29:1604799. DOI
28. Yu Y, Zhang Q, Liu B, Lee JY. Synthesis of nanocrystals with variable high-index Pd facets through the controlled heteroepitaxial growth of trisoctahedral Au templates. *J Am Chem Soc* 2010;132:18258-65. DOI PubMed
29. Sun S, Zhang X, Cui J, Yang Q, Liang S. High-index faceted metal oxide micro-/nanostructures: a review on their characterization, synthesis and applications. *Nanoscale* 2019;11:15739-62. DOI
30. Rosen J, Hutchings GS, Lu Q, et al. Mechanistic insights into the electrochemical reduction of CO_2 to CO on nanostructured Ag surfaces. *ACS Catal* 2015;5:4293-9. DOI
31. Dong JC, Su M, Briega-Martos V, et al. Direct *in situ* raman spectroscopic evidence of oxygen reduction reaction intermediates at high-index Pt(*hkl*) surfaces. *J Am Chem Soc* 2020;142:715-9. DOI
32. Yin Y, Alivisatos AP. Colloidal nanocrystal synthesis and the organic-inorganic interface. *Nature* 2005;437:664-70. DOI PubMed
33. Yang Y, Zhang J, Wei Y, et al. Solvent-dependent evolution of cyclic penta-twinned rhodium icosahedral nanocrystals and their enhanced catalytic properties. *Nano Res* 2018;11:656-64. DOI
34. Liang H, Jiang X, Qi Z, et al. Hematite concave nanocubes and their superior catalytic activity for low temperature CO oxidation. *Nanoscale* 2014;6:7199-203. DOI
35. Liang Y, Shang L, Bian T, et al. Shape-controlled synthesis of polyhedral 50-facet Cu_2O microcrystals with high-index facets. *CrystEngComm* 2012;14:4431-6. DOI
36. Hu S, Tian N, Li M, et al. Trapezohedral platinum nanocrystals with high-index facets for high-performance hydrazine electrooxidation. *Chem Synth* 2023;3:4. DOI
37. Huang L, Liu M, Lin H, et al. Shape regulation of high-index facet nanoparticles by dealloying. *Science* 2019;365:1159-63. DOI
38. Han Y, Zhang X, Cai W, et al. Facet-controlled palladium nanocrystalline for enhanced nitrate reduction towards ammonia. *J Colloid Interface Sci* 2021;600:620-8. DOI
39. Lim J, Liu C, Park J, et al. Structure sensitivity of Pd facets for enhanced electrochemical nitrate reduction to ammonia. *ACS Catal* 2021;11:7568-77. DOI
40. Guo Y, Cai X, Shen S, Wang G, Zhang J. Computational prediction and experimental evaluation of nitrate reduction to ammonia on rhodium. *J Catal* 2021;402:1-9. DOI
41. Liu H, Timoshenko J, Bai L, et al. Low-coordination rhodium catalysts for an efficient electrochemical nitrate reduction to ammonia. *ACS Catal* 2023;13:1513-21. DOI
42. Katsounaros I, Figueiredo MC, Chen X, Calle-vallejo F, Koper MT. Interconversions of nitrogen-containing species on Pt(100) and Pt(111) electrodes in acidic solutions containing nitrate. *Electrochimica Acta* 2018;271:77-83. DOI
43. Molodkina EB, Botryakova IG, Rudnev AV, Ehrenburg MR. Redox-transitions in NO/NH_3 adlayers on a Pt(111) electrode in an acidic solution. *Electrochimica Acta* 2023;444:141997. DOI
44. Hu T, Wang C, Wang M, Li CM, Guo C. Theoretical insights into superior nitrate reduction to ammonia performance of copper catalysts. *ACS Catal* 2021;11:14417-27. DOI
45. Fu Y, Wang S, Wang Y, et al. Enhancing electrochemical nitrate reduction to ammonia over Cu nanosheets via facet tandem catalysis. *Angew Chem Int Ed Engl* 2023;62:e202303327. DOI
46. Hu Q, Qin Y, Wang X, et al. Reaction intermediate-mediated electrocatalyst synthesis favors specified facet and defect exposure for efficient nitrate–ammonia conversion. *Energy Environ Sci* 2021;14:4989-97. DOI
47. Zhong W, Gong Z, He Z, et al. Modulating surface oxygen species via facet engineering for efficient conversion of nitrate to ammonia. *J Energy Chem* 2023;78:211-21. DOI
48. Yao Q, Chen J, Xiao S, Zhang Y, Zhou X. Selective electrocatalytic reduction of nitrate to ammonia with nickel phosphide. *ACS Appl Mater Interfaces* 2021;13:30458-67. DOI
49. Crawford J, Yin H, Du A, O'Mullane AP. Nitrate-to-ammonia conversion at an InSn-enriched liquid-metal electrode. *Angew Chem Int*

Ed Engl 2022;61:e202201604. DOI PubMed PMC

50. Zhang Y, Chen X, Wang W, Yin L, Crittenden JC. Electrocatalytic nitrate reduction to ammonia on defective Au_1Cu (111) single-atom alloys. *Appl Catal B Environ* 2022;310:121346. DOI
51. Yin H, Peng Y, Li J. Electrocatalytic reduction of nitrate to ammonia via a Au/Cu single atom alloy catalyst. *Environ Sci Technol* 2023;57:3134-44. DOI
52. Chen L, Xie A, Lou Y, Tian N, Zhou Z, Sun S. Electrochemical synthesis of tetrahexahedral Cu nanocrystals with high-index facets for efficient nitrate electroreduction. *J Electroanal Chem* 2022;907:116022. DOI
53. Liu F, Chen C, Jiang X, et al. High-index surface structure engineering of Au–Pd concave triple-octahedrons for boosting electrocatalytic nitrate reduction to ammonia. *ACS Sustain Chem Eng* 2023;11:1631-7. DOI
54. Li S, Ma P, Gao C, et al. Reconstruction-induced NiCu-based catalysts towards paired electrochemical refining. *Energy Environ Sci* 2022;15:3004-14. DOI